Current Research in Physiology 3 (2020) 20–29

Contents lists available at ScienceDirect

Current Research in Physiology

journal homepage: www.editorialmanager.com/crphys/Default.aspx

Instant activation of TRP channels by NH_4^+ promotes neuronal bursting and glutamate spikes in CA1 neurons

Saju Balakrishnan, Sergej L. Mironov *

Institute of Neuro- and Sensory Physiology, Georg-August-University, Humboldtallee 23, 37073, Göttingen, Germany

ARTICLE INFO

Keywords:
Hippocampus
Mouse
Glutamate imaging
Bursting
ASIC
TRPC1
TRPV1 channels

ABSTRACT

Ammonia (NH_4^+) is a by-product of cell metabolism and may elicit subcellular effects with specific physiological responses. Chronic effects have been implicated in several neurological diseases and attributed to persistent elevation in blood ammonia levels transferred to the brain. In previous studies the activities of neurons and astrocytes have been examined at ammonia concentrations an order of magnitude higher than measured in the blood. The effects developed within several minutes. Here we focused upon acute responses of neurons to ammonia and whether they may occur at much lower doses. To this end, we combined patch-clamp in CA1 neurons with glutamate imaging in hippocampal slices. Particular attention was paid to the Rett syndrome that has been originally attributed to hyperammonemia. We compared the responses in the wild-type (WT) and model Rett mice (MECP2-null, RTT) to ammonia doses from 0.3 mM on. In both preparations NH_4^+ promptly depolarized neurons and increased the ambient glutamate. The bursting activity emerged in WT and it was augmented in RTT. Searching for subcellular mechanisms we examined possible modulation of ion channels by ammonia. We did not find any changes in HCN- and Ca^{2+} currents, which substantially contribute to the bursting activity. The non-selective cation channels were markedly potentiated by ammonia. ASIC channels had a major contribution to the augmentation of neuronal activity by ammonia. Interestingly, their general blocker amiloride (100 μM) moderately excited CA1 cells akin to NH_4^+. In its presence subsequent ammonia effects were markedly compromised. Blockade of TRPC1 channels partially occluded NH_4^+ effects. ASIC and TRPC1 blockers decreased the amplitude of excitatory postsynaptic currents (EPSC) and neuronal bursts, congruent with a postsynaptic location of the channels. Inhibition of TRPV1 channels potentiated the responses to NH_4^+. EPSC amplitudes did not change, but the frequency decreased, indicating presynaptic effects. All extracellular NH_4^+ actions were observed at concentrations as low as 0.3 mM and the neurons reacted immediately after ammonia arrived the slice. We propose that a brief augmentation of neuronal activity by NH_4^+ may occur either spontaneously during arousal or induced by inhalation of smelling salts.

1. Introduction

Ammonia (NH_4^+) is the main end product of the metabolism of amino acids in the body. Previously, most attention has been attracted to its toxic actions. Millimolar concentrations of NH_4^+ are known to induce various pathological disorders within the brain (Cagnon & Braissant, 2007). The toxicity is often observed during hepatic encephalopathy, when brain NH_4^+ is elevated through circulation. Symptoms such as lethargy and epilepsy are already observed at 0.5 - l.0 mM blood ammonia levels (Yamamoto et al., 2013). Severe CNS disturbances, such as coma, require brain concentrations between 2.5 and 5 mM (Szerb & Butterworth, 1992). The blood ammonia may not match CNS levels, however. Many biochemical reactions can either produce NH_4^+ or utilize it as a substrate that could potentially induce fast and big local ammonia changes within the brain. The considerations have been recently cast into a hypothesis treating brain ammonia as a potential neurotoxic factor in Alzheimer's (Seiler, 2002; Adlimoghaddam et al., 2016). Changes in ammonia levels due to the intracellular metabolism of amino acids is thought to proceed mostly in the glia, which perhaps explains why the majority of studies have been focused upon astrocytes (Bachmann, 2002; Rose et al., 2005; Marcaggi & Coles, 2001; Rangroo Thrane et al., 2013; Halpin et al., 2014; Schroeter et al., 2015; Oja et al., 2017). The long-term actions of ammonia documented in these studies appealed to various mechanisms e. g. a disturbed equilibrium between glutamate and

* Corresponding author.
E-mail address: smirono@gwdg.de (S.L. Mironov).

https://doi.org/10.1016/j.crphys.2020.05.002
Received 5 March 2020; Received in revised form 11 May 2020; Accepted 24 May 2020

glutamine and induction of glia swelling; Ca-mediated efflux of glutamate from astrocytes; impairment of mitochondrial function with production of reactive oxygen species, including NO. All these effects rely upon specific signaling cascades that could match a considerable delay in onset and overlong duration of responses (from several minutes to hours). A suggested attribution of NH_4^+ effects to astrocytes nonetheless requires understanding whether and how ammonia can directly modify the properties of neurons.

Previous studies in hippocampus (reviewed in (Szerb & Butterworth, 1992)) indicated modulation of neuronal and synaptic activities by ammonia, albeit at supramillimolar concentrations and chronic challenges. The effects are mostly inhibitory and attributed to slow depolarization by ammonia, promoting inactivation of sodium conductance.

The data cannot explain immediate stimulating action of ammonia vapors, whose inhalation was used historically for arousal after fainting. Such sudden increases in neuronal activity should be mediated by specific mechanisms that are still elusive but may help to clarify the well-documented both positive and toxic effects of hyperammonemia. The data about subcellular targets of NH_4^+ are scarce. It is known that ammonia directly activates acid-sensitive ion channels (ASIC), (Mironov & Lux, 1993; Pidoplichko & Dani, 2006) and transient receptor potential (TRP) channels TRPV1 and TRPC1 (Dhaka et al., 2009; Saffarzadeh et al., 2016). However, the use of cultured cells limits a functional significance of these studies.

We aimed to examine acute ammonia effects in the intact neuronal tissue. To this end, we monitored the activity of hippocampal CA1 neurons using the whole-cell patch-clamp technique and measured ambient glutamate with fluorescent sensor iGluSnFr targeted to the membrane of neurons or astrocytes. As in the previous studies (Balakrishnan & Mironov, 2018a; Balakrishnan & Mironov, 2018b; Balakrishnan & Mironov, 2018), we routinely compared the responses in slices from the wild-type (WT) mice and animals carrying the Rett Syndrome (RTT) deficiency. The rationale was to seek for possible differences in responses to NH_4^+ in RTT and WT to ammonia, because the Rett Syndrome has been originally attributed to hyperammonemia (Rett, 1966). A direct connection in patients was examined in only one study (Campos-Castelló et al., 1988) and no significant changes in blood ammonia in RTT patients have been found. The question remains, because ammonia levels in blood and the brain do not mirror each other (Marcaggi & Coles, 2001).

Rett Syndrome is a neurodevelopmental disorder that causes improper maturation of the synapses due to the loss of function of methyl-CpG binding protein 2, MeCP2 (Moretti & Zoghbi, 2006). The hyperexcitability in RTT is thought to stem from excitation/inhibition imbalance (Zhang et al., 2008) and related to abnormal glutamate handling (Johnston et al., 2014). We indeed measured elevated ambient glutamate levels in RTT (Balakrishnan & Mironov, 2018a). This apparently set conditions to produce regenerative glutamate spikes that were typical in RTT hippocampus, and virtually absent in WT (Balakrishnan & Mironov, 2018a; Balakrishnan & Mironov, 2018b; Balakrishnan & Mironov, 2018). Glutamate spikes in WT readily emerged only after activation of metabotropic glutamate receptors (mGluR) (Balakrishnan & Mironov, 2018).

We here report that NH_4^+ excites CA1 neurons, elevates ambient glutamate, enhances bursting activity and induces glutamate spikes in WT. The effects in RTT are similar but have bigger amplitudes and longer durations. Importantly, we consistently observed the effects already at 0.3 mM NH_4^+, an order of magnitude lower than used in other studies (Cagnon & Braissant, 2007; Szerb & Butterworth, 1992; Bachmann, 2002; Oja et al., 2017). Patch-clamp studies revealed no modifications of voltage-sensitive HCN- and Ca^{2+} channels after ammonia. To find an explanation of increased excitability by ammonia we turned to non-selective ASIC, TRPC1 and TRPV1 channels. They were activated by NH_4^+ and correspondingly modulated neuronal and synaptic properties. Their concerted actions converge to transiently enhance neuronal and glutamate activities after brief ammonia surges. Because glutamatergic neurons endorse the biggest population within the brain, similar responses to NH_4^+ may be expected to occur elsewhere, adding a broader implication to the presented findings.

2. Methods

All experimental procedures used are essentially the same as employed in previous studies (Balakrishnan & Mironov, 2018a; Balakrishnan & Mironov, 2018b; Balakrishnan & Mironov, 2018) and only briefly recapitulated below.

2.1. Preparation and solutions

All mouse experiments were approved by the local authority, the Lower Saxony State Office for Consumer Protection and Food Safety (Niedersächsisches Landesamt für Verbraucherschutz und Lebensmittelsicherheit) and performed in accordance with the issued guidelines and regulations. For removal of tissues, animals were deeply anaesthetized and rapidly killed by cervical dislocation. All experiments were performed using the mouse model for Rett Syndrome (further RTT); strain B6.129P2(C)– MeCP2tm1-1Bird (Guy et al., 2001) from the Jackson Laboratory (Bar Harbor, ME, USA). After preparation all mice were routinely genotyped to confirm the wild-type (WT) and MECP2-null (RTT) mice.

Transverse hippocampal slices were prepared at postnatal day P3 and placed on the support membranes (Millicell-CM Inserts, PICMORG50; Millipore). Slices for experiments were virally transduced with glutamate sensor (Marvin et al., 2013) that was targeted to neurons (AAV5.hSyn.iGluSnFr.WPRE.SV40) or astrocytes (AAV5.GFAP.iGluSnFr.WPRE.SV40). The constructs were from Penn Vector Core, Department of Pathology and Laboratory Medicine; U. Pennsylvania. Transduction was done two days after plating slices and the experiments were performed from P7 on, after expression of the sensor reached the steady state. The probes targeted to the glia and neurons reported similar changes in all experimental protocols used, see also (Balakrishnan & Mironov, 2018a; Balakrishnan & Mironov, 2018b; Balakrishnan & Mironov, 2018). Because the sensors are expressed in the plasma membranes of neurons or astrocytes and exposed to the thin extracellular space (<100 nm wide), they should sense the same ambient glutamate. The data obtained with the two sensors were therefore pooled together for analysis.

In the experiments, the support membrane with the attached slice was placed in the recording chamber. It was continuously superfused at 34 °C with artificial cerebrospinal fluid (ACSF) contained (in mM): 138 NaCl, 5 KCl, 1.5 $CaCl_2$, 1 $MgCl_2$, 30 HEPES, 1 NaH_2PO_4, 10 glucose, and pH 7.4, adjusted with NaOH. In the experiments with NH^+_4 elevated above 1 mM, Na^+ levels were correspondingly lowered to maintain osmolality. All salts and other common substances were from Sigma (Deisenhofer, Germany). The agonists and antagonists for channels and receptors were from Tocris Bioscience (Bristol, UK) and Alomone Labs (Israel). The stock solutions of drugs were made either in DMSO or ACSF and diluted at least by 1000-fold for applications.

2.2. Imaging

The cells were viewed under a 40× objective (Achroplan, N. A. 0.95) in a Zeiss Axioscope equipped with a monochromatic light source (CAIRN, UK). Images from a cooled CCD camera (ANDOR) were digitized (256×256 pixels at 12 bit resolution) and collected with ANDOR software. Metamoph (Princeton Instruments) was used for analysis. In glutamate imaging the cells were illuminated at 470 nm and the emission was collected at 525 ± 10 nm. Glutamate levels were obtained from relative increases in fluorescence $\Delta F/F_o$ as described (Balakrishnan & Mironov, 2018a). A typical experimental configuration is depicted in the inset in Fig. 1.

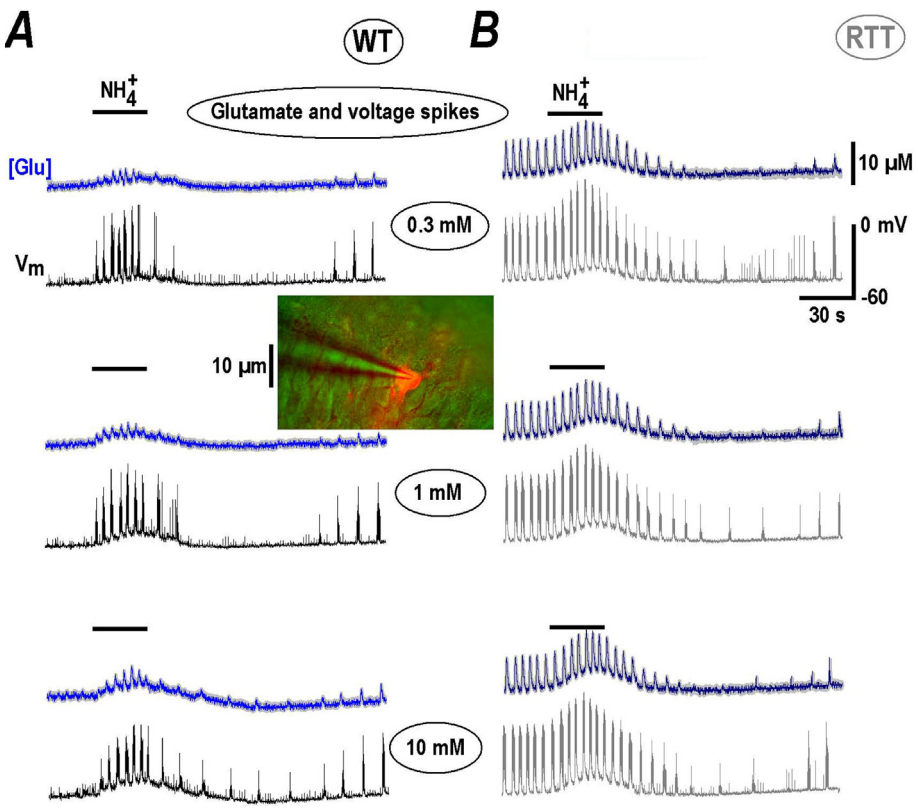

Fig. 1. NH_4^+ transiently increases ambient glutamate and neuronal bursting in CA1 neurons. **A** and **B** show the effects of NH_4^+ in slices prepared from wild-type (WT) and model Rett animals (RTT) as indicated. Each column presents the three panels containing the two traces showing the changes in ambient glutamate (blue) and voltage trajectories (black) measured simultaneously. Mean [Glu] traces were obtained from 12 regions of interest encircled the cells expressing glutamate sensor iGluSnFr (see Methods). Average traces are overlaid onto grey background showing ± SEM. The slice was transduced with neuronal glutamate sensor and CA1 neuron was selected to patch. The inset in the middle shows the experimental configuration. The internal solution contained Alexa 588 to visualize the neuron with dendritic tree (red). We consistently observed the repetitive glutamate spikes in naïve slices from RTT animals (**B**). Application of NH_4^+ for 30 s at 0.3–10 mM (as indicated) induced stereotypic effects consisted of brief augmentation of activity with subsequent depression. The glutamate spikes coincided with burst discharges in neurons (presented as black and grey traces in respective panels). In naïve slices from WT animals (**A**) repetitive glutamate spikes were absent and emerged with NH_4^+ addition. The responses were similar but had smaller amplitude. During wash-out and slow recovery ambient glutamate levels slightly elevated that was followed by appearance of glutamate spikes in WT. The mean data are summarized in Fig. 2.

2.3. Patch-clamp

Recording electrodes were pulled from borosilicate glass (WPI, Berlin, Germany) and had resistances of 2–3 MΩ. In current-clamp recordings the pipettes were filled with a solution containing 110 mM K^+-gluconate, 5 mM KCl, 50 mM HEPES, 0.005 mM EGTA, 4 mM $MgSO_4$, 4 mM ATP, 0.2 mM GTP, 9 mM phosphocreatine, at pH 7.4 adjusted with KOH. In recording HCN and Ca^{2+} currents, we used a Cs^+ based solution containing 92 mM $CsMeSO_4$, 43 mM CsCl, 5 mM TEA-Cl, 0.4 mM EGTA, 1 mM $MgCl_2$, 10 mM HEPES, 4 mM ATP, 0.4 mM GTP, at pH 7.4 adjusted with CsOH. The osmolality was 290 ± 5 mosm.

Patch-clamp signals were recorded with an EPC-9 (HEKA, Germany) amplifier. HCN and Ca^{2+} currents were evoked by voltage steps to −110 and −40 mV for 300 ms, respectively, from a holding potential of −70 mV (close to the resting potential measured in CA1 neurons). Although HCN currents might be better evoked from a holding potential which is more positive than −60 mV to assure their complete deactivation (Mironov et al., 2000), we have chosen −70 mV as a holding potential on the following grounds: At −50 mV, the Ca^{2+} conductance is small, but cannot be neglected (Balakrishnan & Mironov, 2018a; Balakrishnan & Mironov, 2018b; Balakrishnan & Mironov, 2018). The persistent Ca^{2+} current can steadily elevate intracellular calcium and produce unwanted side effects. Activation of HCN channels achieves 95% at −110 mV (Balakrishnan & Mironov, 2018b; Mironov et al., 2000) and we avoided bigger hyperpolarization steps to keep neurons viable.

The analysis of spontaneous postsynaptic potentials (sEPSC) was performed as described previously (Mironov & Langohr, 2007). In brief summary, we calculated the first two moments $m_n = \int I^n(t)dt$ of the continuous 10 s-long-recordings of the current $I(t)$ at −70 mV with bursting periods excluded. The mean amplitude (A) and frequency of synaptic currents (f) were determined as $A = 4\tau m_2/m_1$ and $f = m^2/4\tau m_1$, where τ is a decay constant of the mean EPSC, obtained from single non-overlapping EPSCs showing the fast rise time.

2.4. Statistics

Approximately equal numbers of neurons were measured in parallel, both for the wild-type and MeCP2-null mice, and analyzed blinded to genotype. Each test in this study was repeated with at least four different preparations and the mean data in imaging were obtained by analyzing responses for >12 cells present in the image field. The mean traces in time-lapse experiments that present sample responses are overlaid upon thick grey areas showing SEM obtained from single traces. Means ± SEM were compared by using Student's t test, with $p < 0.05$ being the criterion for statistical significance. The results of independent experiments were compared with a Mann-Whitney-U-test.

3. Results

Brief application of ammonia to the hippocampal slices readily increased ambient glutamate and potentiated bursting activity. The responses in CA1 area were stereotypical in the preparations from both wild-type and RTT animals (Fig. 1). They were observed already at 0.3 mM NH_4^+ and showed saturation at 10 mM NH_4^+ as summarized in Fig. 2. At 30 mM NH_4^+ the effects were essentially the same as at 10 mM NH_4^+ ($n = 3$, for both WT and RTT, data not shown). For all concentrations tested, NH_4^+ induced a transient increase in ambient glutamate and neuronal activity, shown in Fig. 1 by the blue and black/grey traces, respectively. The repetitive glutamate spikes are tightly related to the bursting activity in RTT preparations (Balakrishnan & Mironov, 2018a; Balakrishnan & Mironov, 2018b; Balakrishnan & Mironov, 2018) and both activities slices were potentiated by NH_4^+ (Fig. 1B). In the majority of naïve WT slices the rhythmic activity was absent and NH_4^+ induced transient appearance of glutamate spikes and bursts (Fig. 1A). Wash-out of ammonia produced slight depolarization that paralleled the increase in ambient glutamate, and regenerative glutamate transients established. The effects remind of the appearance of rhythmic activity in WT slices after stimuli that elevated ambient glutamate (Balakrishnan & Mironov,

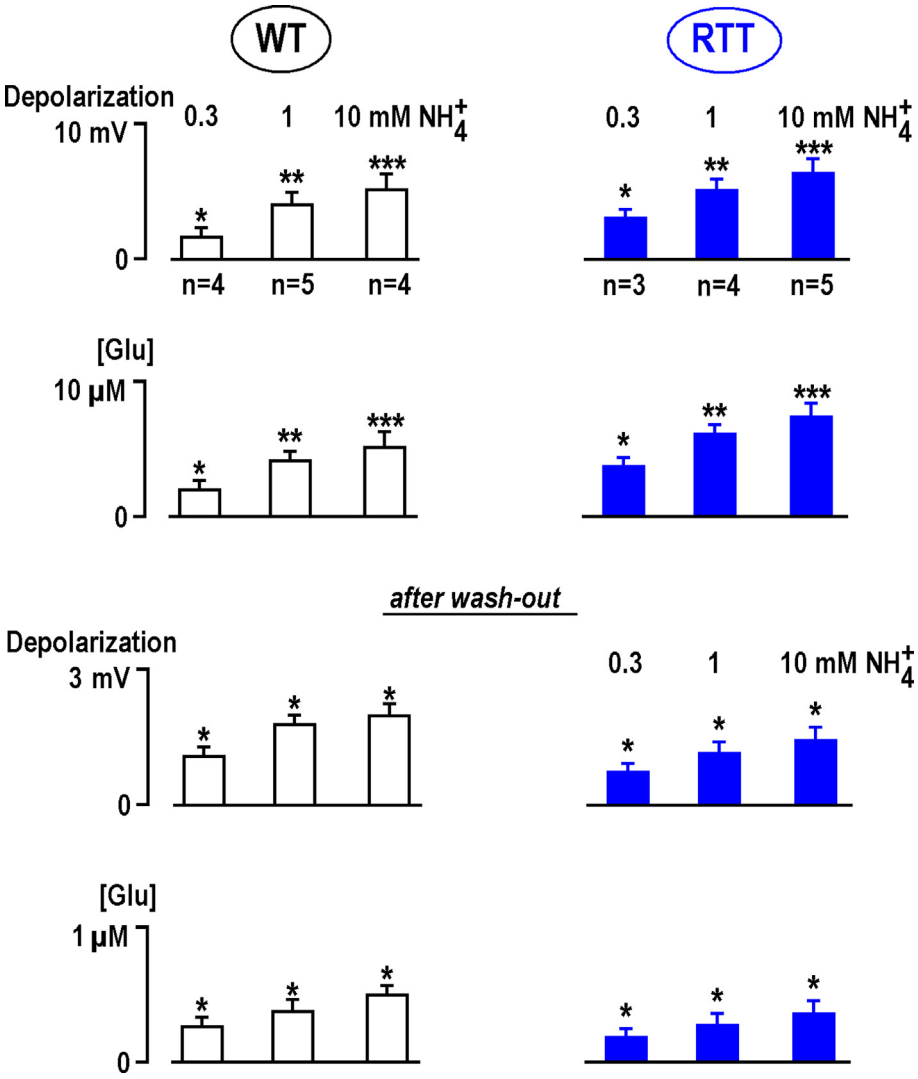

Fig. 2. Changes in ambient glutamate and depolarization by NH_4^+ in CA1 neurons in the slices from wild-type and RTT animals. All data were obtained from experiments made in different fresh (naive) preparations from RTT and WT animals as indicated. Group summary presents mean data ± SEM from experiments whose number is indicated in the first row. The differences from the baseline (first three rows) are significant at $p < 0.1$ (*), $p < 0.05$ (**), and $p < 0.01$ (***) (Student's *t* test). Note that the amplitude of responses showed saturation with increasing NH_4^+ concentration. Estimation of EC_{50} from mean data at three different concentration gave 2.4 (WT) and 2.6 mM (RTT), respectively. The data obtained in WT and RTT at 0.3 and 1 mM NH_4^+ are significantly different at $P < 0.01$. The differences between the means for 1 and 10 mM NH_4^+ are different at $P < 0.1$ (*P* estimates were obtained using Mann-Whitney-*U*-test).

2018). The analysis of NH_4^+ effects in WT and RTT are summarized in Fig. 2 with statistical significance indicated.

Depolarization and concomitant enhancement of neuronal excitability implies the activation of some cation channels that mediate inward current. The first candidates to examine are the voltage-sensitive Ca^{2+} (I_{Ca}) and hyperpolarization-activated currents (I_{HCN}), which contribute to the bursting activity. The channels have different characteristics in WT and RTT CA1 neurons (Balakrishnan & Mironov, 2018a; Balakrishnan & Mironov, 2018b; Balakrishnan & Mironov, 2018); and we asked whether they can be modulated by NH_4^+. I_{Ca} and I_{HCN} currents characteristics before and after NH_4^+ applications showed no significant differences (Fig. 3). In these experiments we concerned possible modulation of I_{Ca} and $I_{HCN\ by}$ intracellular pH (pH_i) as reported in (Mironov & Lux, 1991; Zong et al., 2001), respectively. Intracellular alkalinization develops within several minutes (Mironov & Lux, 1991). The absence of changes in the I_{Ca} and I_{HCN} currents after NH_4^+ for 30 s applications indicates an exclusively extracellular target in our experiments.

We next tested the non-selective channels that can generate the inward current we sought. The first choice was acid-sensitive ion channels (ASIC) that are activated by NH_4^+ (Mironov & Lux, 1993; Pidoplichko & Dani, 2006). Unexpectedly, a general ASIC blocker, amiloride, produced responses akin to NH_4^+ (Fig. 4A, the two traces on the left). After brief initial potentiation, the glutamate spikes and neuronal bursts diminished, but persisted (group summary of effects of amiloride and other TRP blockers is presented in Fig. 5). The addition of NH_4^+ in the presence of amiloride (Fig. 4A, on the right) elicited much smaller responses compared to the 'control' responses (Fig. 1) indicating a substantial blockade of ASIC channels by amiloride. This dichotomous action can be explained by the results of Adams et al. (1999) who showed that amiloride can act as an agonist and antagonist of ASIC channels. This feature should be taken into account in possible clinical applications, because the drug may produce a weak stimulating effect opposite to a presumed inhibitory action. Amiloride also decreased the amplitude of spontaneous excitatory postsynaptic currents (EPSC) and synaptic drives (a correlate of neuronal bursts) (Fig. 4B). No significant changes in frequency of EPSCs was observed (Fig. 5A), indicating only postsynaptic effects.

Several TRP channels can be modulated by NH_4^+ (Dhaka et al., 2009; Saffarzadeh et al., 2016). TRPC1 channel blocker, 20 µM SKF96365 (1-[2-(4-Methoxyphenyl)-2-[3-(4-methoxyphenyl) propoxy] ethyl-1-*H*-imidazole hydrochloride) significantly decreased the amplitude and frequency of glutamate spikes and neuronal bursts (Fig. 6A; Fig. 5B). 1 mM NH_4^+ induced transient potentiation of activity (Fig. 6A, on the right), significantly smaller than the control responses (Fig. 1). SKF decreased the amplitudes of EPSC and synaptic drives, and the EPSC frequency was unchanged (Fig. 5B). The mean EPSCs after SKF became 30% smaller (the two traces in Fig. 6B on the right). The decay time was not significantly changed (3.6 ± 0.4 vs. 3.8 ± 0.3 ms after SKF, $p > 0.1$) which indicates unchanged electrotonic length i. e. the active TRPC1 channels postsynaptically located in the spines but not within the dendritic shaft.

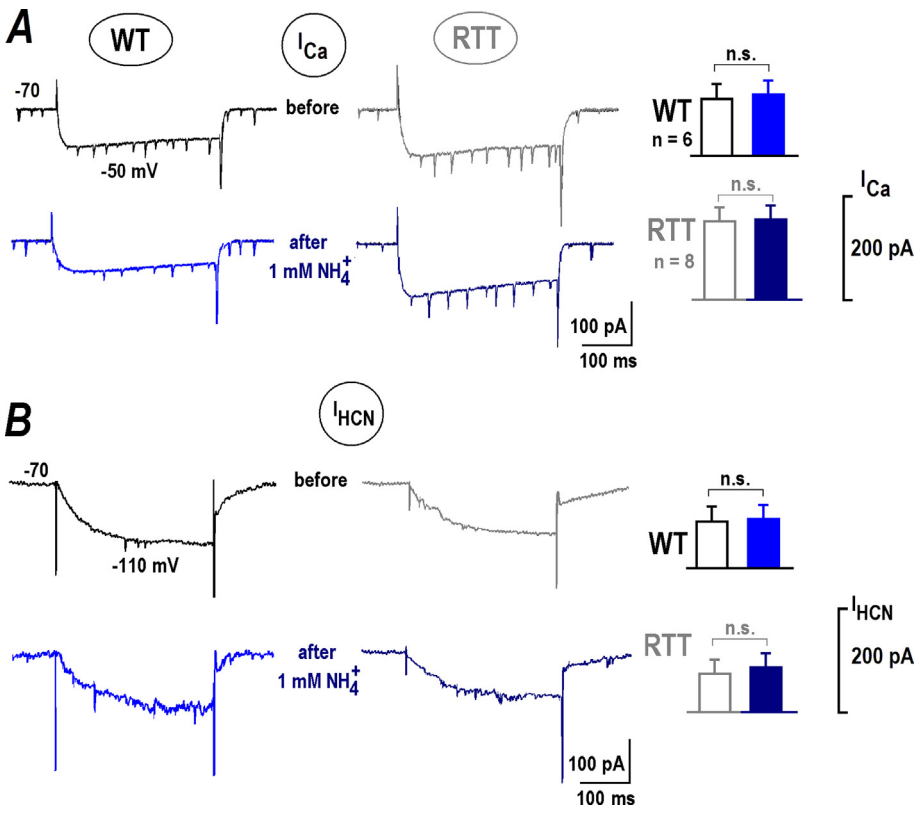

Fig. 3. NH_4^+ does not modulate voltage-sensitive Ca^{2+} (I_{Ca}) and hyperpolarization-activated (I_{HCN}) channels. Whole-cell voltage-clamp experiments were made in CA1 neurons from WT and RTT animals as indicated. **A** – Sample I_{Ca} traces were measured for 300 ms-long voltage steps from −70 to −50 mV before and 30 s after application of 1 mM NH_4^+. **B** – Sample I_{HCN} traces were obtained in the same cells with voltage steps from −70 to −110 mV. The histograms on the right present group summary. The Student's *t* test in all cases gave $p > 0.1$ that indicated not significant (n.s.) differences. I_{Ca} currents in WT were yet distinctly bigger (−111 ± 7 vs. −191 ± 12 pA) and I_{HCN} currents were significantly smaller in RTT (−121 ± 8 vs. −81 ± 6 pA). For both sets of data $P < 0.1$ (the Mann-Whitney-*U*-test).

TRPC1 channels can cross-talk to metabotropic glutamate receptors (mGluR). This signaling pathway is important in CA1 (Balakrishnan & Mironov, 2018) and other neurons (Lepannetier et al., 2018). Stimulation of mGluR1/5 with DHPG ((S)-3,5-Dihydroxyphenylglycine) in slices from WT animals induced regenerative glutamate spikes and neuronal bursts (Fig. 7A). The responses to NH_4^+ after DHPG in WT became bigger than in naïve slices (compare Figs. 1A and 7A, group summary is given in Fig. 5D). EPSCs after DHPG became bigger and faster (Fig. 7B). This can be explained by the reduction of I_{HCN}-mediated shunting in CA1 dendrites after mGluR1 stimulation (Balakrishnan & Mironov, 2018).

TRPV1 (vanilloid) channels contribute to NH_4^+ effects in sensory neurons (Dhaka et al., 2009). We tested a specific blocker BCTC (4-(3-Chloro-2-pyridinyl)-N-[4-(1, 1-dimethylethyl) phenyl]-1-piperazinecarboxamide). It has a high potency ($IC_{50} = 35$ nM) (Jardín et al., 2017) and 1 μM BCTC fully blocked TRPV1 channels in DRG cells (Kitamura et al., 2018) and inhibited TRPV1 channels expressed in HEK293t cells at 100 nM by 98% (Leffler et al., 2008). In our experiments 20 μM BCPC reliably increased the amplitude and frequency of neuronal bursts and related glutamate transients in RTT. Subsequent application of 1 mM NH_4^+ produced bigger effects than in the control (Fig. 8A on the right vs. Fig. 1B, group summary in Fig. 5D). In the presence of BCTC the frequency of EPSC increased and the amplitudes of spontaneous and mean EPSC did not change (Figs. 5 and 6B), which indicates a presynaptic target.

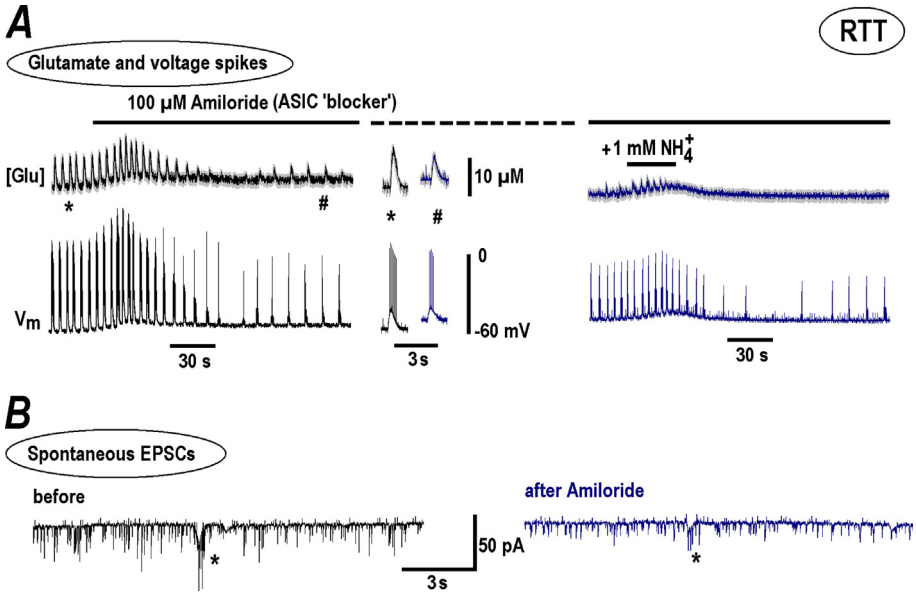

Fig. 4. Amiloride modulates NH_4^+ effects n RTT slices. The recordings were made in RTT slices that showed spontaneous glutamate spikes related to AP bursts in CA1 neurons. **A** – The two traces show changes in ambient glutamate (top) and the voltage trajectories in CA1 neuron (bottom). In this experiment 100 μM amiloride (a general blocker of ASIC channels) was first applied to the bath and then 1 mM NH_4^+ was added. The recordings on the left show that amiloride alone acted akin NH_4^+ (Fig. 1). The two insets in the middle present glutamate spikes and neuronal bursts before and after amiloride effect stabilized. The episodes in the continuous traces on the left were taken at time-points marked by asterisk and hash symbols. In the presence of amiloride a subsequent addition of NH_4^+ elicited much smaller effects than in the control (compare the traces on the right and 'a standard response' in Fig. 1B). **B** – Spontaneous EPSCs. The synaptic drives are indicated by asterisks. The recordings were made in the whole-cell voltage-clamp mode at the holding potential −70 mV. Note small attenuation of amplitudes of EPCS and synaptic drives in the presence of amiloride. The mean data from respective experiments are summarized in Fig. 5.

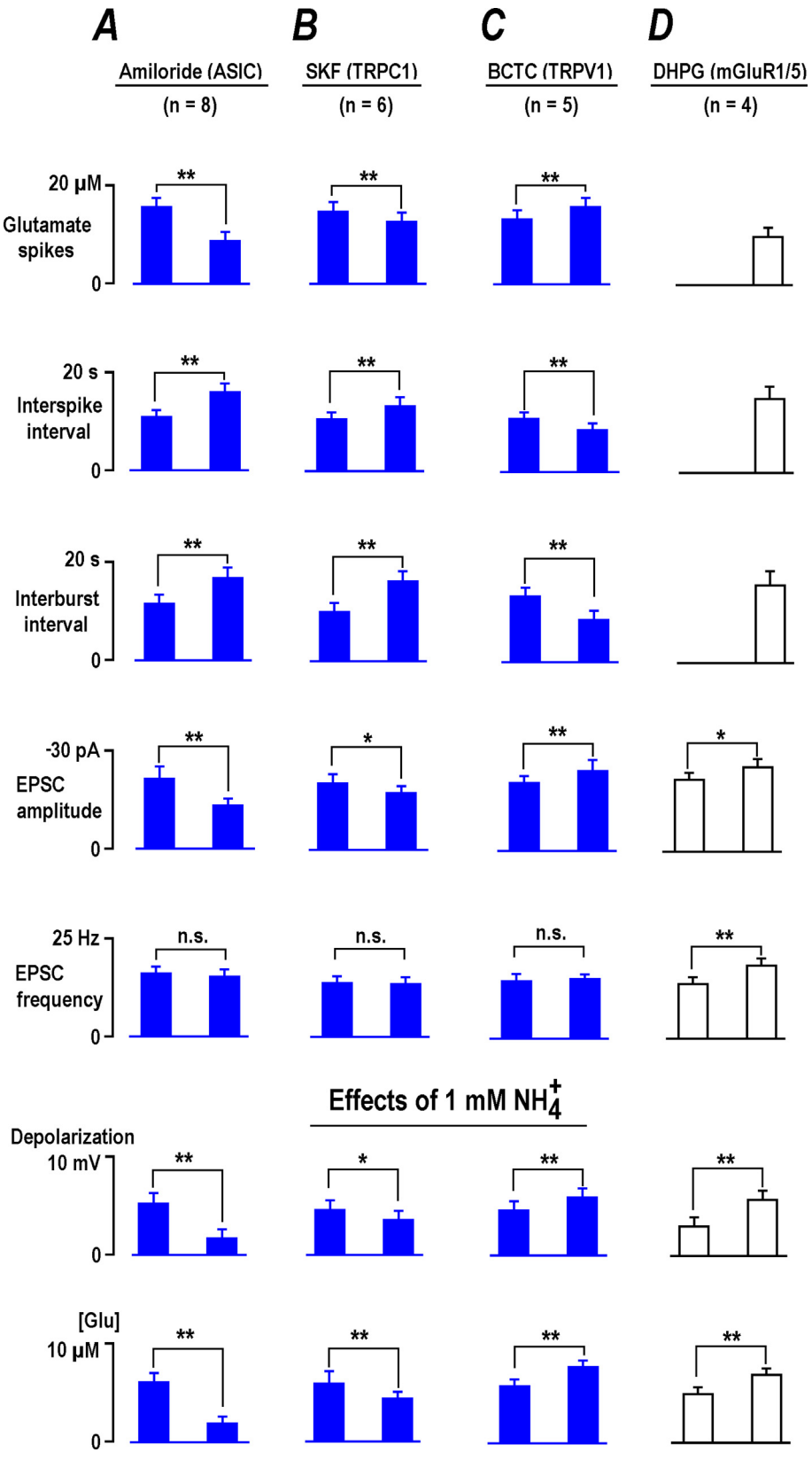

Fig. 5. Effects of channel blockers on basal activity and NH_4^+ responses in CA1 neurons. All data were obtained from experiments made in different fresh (naive) preparations from RTT and WT animals as indicated. The effects of channel blockers were collected largely in RTT (blue bars), because the slices consistently demonstrated spontaneous glutamate transients. To establish them in WT slices we first activated mGluR1/5 with DHPG to establish the stable rhythmic activity (Balakrishnan & Mironov, 2018), and then examined the response to NH_4^+ as shown also in Fig. 7. Group summaries present mean data ± SEM from the experiments whose number is listed in each column at the top. In all tests, the mean intervals between glutamate spikes were close to interburst periods ($p > 0.1$, Student's t test). The effects of blockers showed significant differences at $p < 0.1$ (*), $p < 0.05$ (**), or were not significant ($p > 0.1$, n. s.) (Student's t test) and are correspondingly marked in the histograms.

4. Discussion

NH_4^+ in the brain has a plethora of actions; all considered as pathological (Cagnon & Braissant, 2007; Yamamoto et al., 2013; Szerb & Butterworth, 1992; Seiler, 2002; Adlimoghaddam et al., 2016; Bachmann, 2002; Rose et al., 2005; Marcaggi & Coles, 2001; Rangroo Thrane et al., 2013; Halpin et al., 2014; Schroeter et al., 2015; Oja et al., 2017). A seminal example is a hepatic encephalopathy that stems from elevation of ammonia levels in the body translated to the CNS, and causing hyperammonemia. The blood ammonia levels may not represent

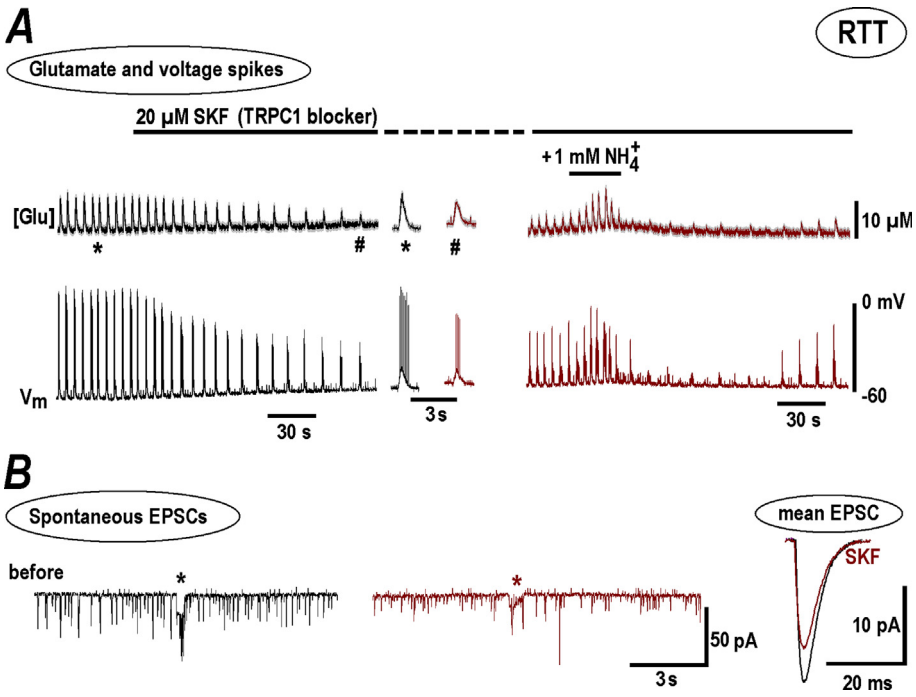

Fig. 6. NH_4^+ effects n RTT slices are diminished in the presence of TRPC1 channel blocker, SKF. The experimental paradigm was similar to that described in Fig. 4. Here also the results for RTT slices with spontaneous activity were used for presentation as they showed spontaneous activity. **A** - SKF suppressed the amplitude and frequency of glutamate spikes and AP bursts (left panel). The two episodes in the middle show sample activities at the expanded time-scale before and after DHPG. The right panel demonstrates a diminished effect of subsequent NH_4^+ application in the presence of SKF. Spontaneous EPSCs and synaptic drives also had smaller amplitudes (**B**). The mean data from respective experiments are summarized in Fig. 5. The traces obtained in the presence of SKF were brown-coded for comparison.

an actual value within the brain (Marcaggi & Coles, 2001). Neurons and glia cells are metabolically active and various biochemical reactions can lead to large and fast regional variations in extracellular ammonia, sensed by specific subcellular entities, producing ultimate changes in the neuronal activity. We sought for mechanisms that may underlie direct ammonia actions on neurons. Chronic NH_4^+ effects in the hippocampus have been studied before, with 'field' macroelectrodes or sharp microelectrodes (Szerb & Butterworth, 1992). We looked 'deeper' and applied patch-clamp in combination with glutamate imaging to monitor the activity of CA1 neurons. We focused upon immediate responses of neurons to low doses of ammonia, which have not been examined in detail.

Specifically, we found that (a) as low as 0.3 mM NH_4^+ depolarizes CA1 neurons; (b) ammonia transiently potentiates neuronal excitability as manifested by enhanced neuronal bursting and repetitive glutamate spikes; (c) the effects are mediated by postsynaptic ASIC and TRPC1 channels and presynaptic TRPV1 channels; (d) in slices from WT animals the responses were similar but distinctly weaker than in RTT (Figs. 1 and 2). Because the majority of CNS neurons are glutamatergic, the responses of CA1 neurons to ammonia may represent stereotypical reactions within the brain.

The fluorescent glutamate sensor iGluSnFr (Marvin et al., 2013) is expressed in the plasma membrane and senses interstitial glutamate

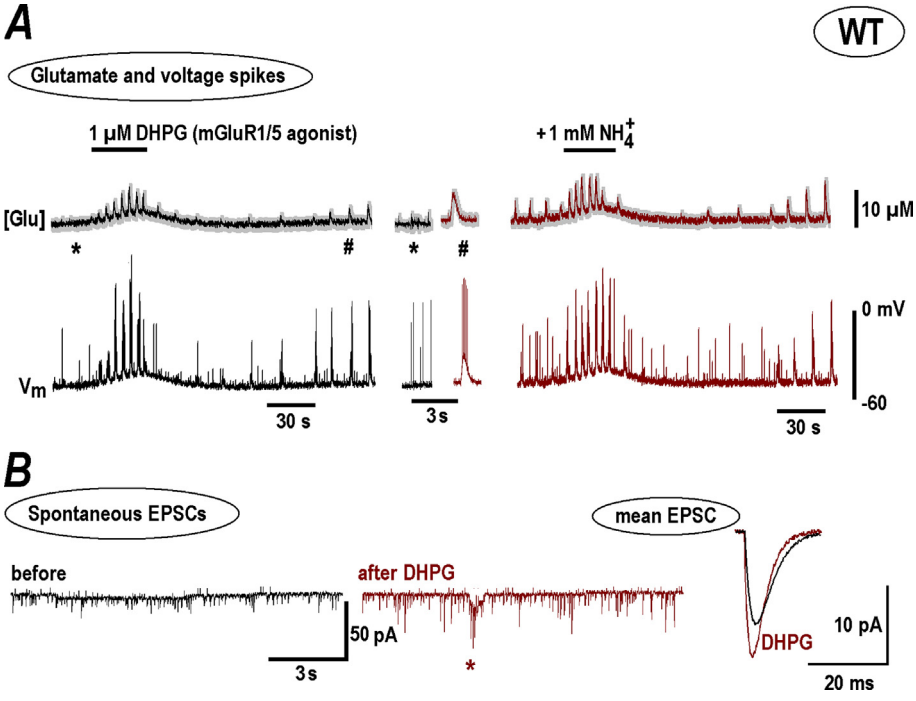

Fig. 7. NH_4^+ effects n WT slices after stimulation of mGluR1/5 with DHPG. **A** – 1 μM DHPG initiated transient appearance of glutamate spikes and neuronal bursts in WT preparation, and, after several minutes wash-out a robust spontaneous activity appeared, in line with previous findings (Balakrishnan & Mironov, 2018). The episodes of activity before and after DHPG are extracted from continuous traces at times indicated by asterisk and hash symbols and shown in the middle at the expanded time-scale. The responses to NH_4^+ then became distinctly bigger after treatment and resembled those recorded in naïve RTT slices (see Fig. 1B for comparison and mean data in Fig. 2). B – Spontaneous EPSCs before and after DHPG. A synaptic drive (a correlate of neuronal burst) is marked by asterisk in the middle trace. Mean EPSCs are shown on the right. They became sharper and bigger after DHPG that can be explained by diminution of I_{HCN}-mediated shunting in dendrites (Balakrishnan & Mironov, 2018).

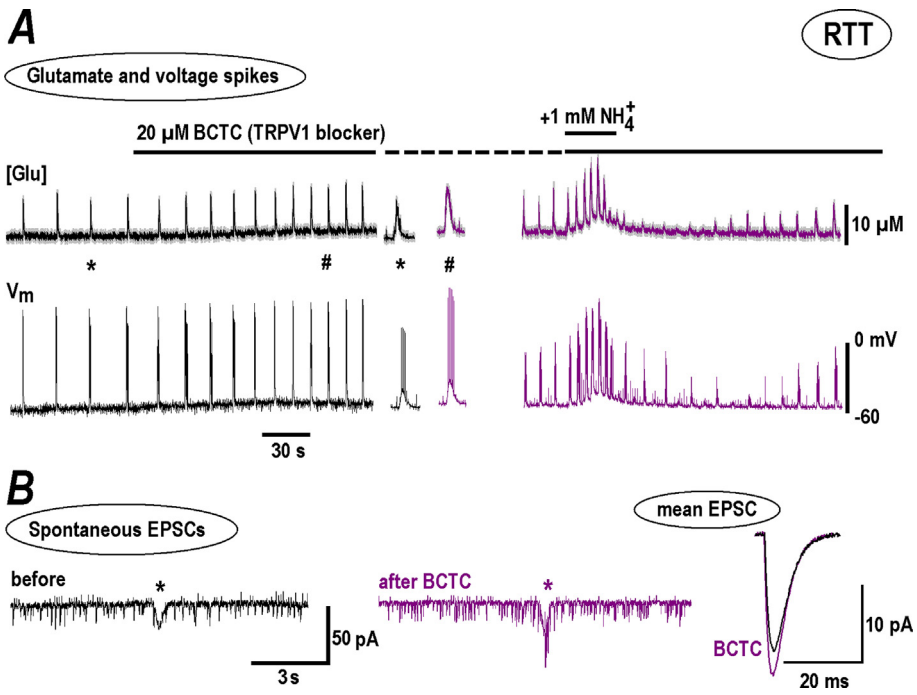

Fig. 8. Modulation of NH_4^+ effects in RTT slices by TRPV1 channel blocker, BCTC. The experiments with BCTC were conducted in a similar way as presented in Figs. 4 and 6 for amiloride and SKF, respectively. **A** – BCTC increased the amplitude and frequency of glutamate spikes and AP bursts (left panel) and potentiated subsequent response to NH_4^+ (right panel). **B** – Continuous traces show spontaneous EPSCs and include single synaptic drive (asterisk). BCTC increased EPSC amplitude and the frequency was unchanged (the statistics is given in Fig. 5). Mean EPSC on the right demonstrate some increase in the amplitude with the time-course unchanged, consistent with unaltered electrotonic conduction. The traces obtained in the presence of BCTC are violet-coded. The mean data from respective experiments are summarized in Fig. 5.

changes from 0.1 μM to 1 mM as fast as 1 ms (Balakrishnan & Mironov, 2018a). Glutamate imaging unraveled a novel hallmark of RTT phenotype in hippocampus - regenerative glutamate spikes that are generated synchronously and tightly related to bursting activity in CA1 neurons (Balakrishnan & Mironov, 2018a; Balakrishnan & Mironov, 2018b; Balakrishnan & Mironov, 2018). Such an activity pattern is presented in Figs. 1, 4, 6 and 8. Low NH_4^+ doses elevated ambient glutamate both in RTT and WT. In RTT slices the spiking activity was enhanced. In naïve WT preparations ammonia induced the glutamate spikes for a short time that then subsided. After several minutes of wash-out repetitive transients reappeared and persisted. This reminds of previously observed effects in WT, where robust rhythmic glutamate spikes in WT are established after brief glutamate surges due to stimulation of mGluR1 (Balakrishnan & Mironov, 2018).

NH_4^+ has a variety of effects upon the cells. For example, it is reported to exert long-term intracellular effects through various biochemical cascades in glia (Cagnon & Braissant, 2007; Bachmann, 2002; Rose et al., 2005; Marcaggi & Coles, 2001; Rangroo Thrane et al., 2013; Halpin et al., 2014; Schroeter et al., 2015; Oja et al., 2017). The data in these studies have been collected at 10-fold bigger concentrations of ammonia that were applied for up to 1 h. The most ubiquitous NH_4^+ action is the ability to alkalinize intracellular pH that modifies the Ca^{2+} (Mironov & Lux, 1991), HCN (Zong et al., 2001), and TRPV1 channels (Dhaka et al., 2009). The changes in pH_i develop within several minutes, even when 10 mM NH_4^+ is applied (Mironov & Langohr, 2007). To assure that the NH_4^+ effects in our experiments are extracellular, the duration of applications was set to a minimum (30 s) and 1 mM NH_4^+ was used in most pharmacological experiments. The absence of distinct changes in I_{Ca} and I_{HCN} (Fig. 2) speaks for solely extracellular ammonia actions under the conditions used.

Ammonia not only diffuses passively through the cell membranes in NH_3 form but can also permeate through ion channels. For example, NH^+_4 permeates around twice better than Na^+ through TRPV3 (Schrapers et al., 2018) and nACh channels (Hille, 2001). In the cytoplasm, NH^+_4 can give away the extra proton and acidify the cell interior. The effects are dubbed as unconventional ammonia actions (Nagaraja & Brookes, 1998; Burckhardt & Frömter, 1992) but not confirmed in other studies (cf. (Marcaggi & Coles, 2001) for review). Let us estimate possible effects in our case. After application of 1 mM NH^+_4 we measured the currents -48 ± 4 pA ($n = 6$, WT) and -52 ± 6 pA ($n = 6$, RTT). They are compatible with that mediated by TRPC1 channels after activation of mGluR1 with DHPG (Balakrishnan & Mironov, 2018). Given a spherical cell with 10 μm radius and intracellular volume of 4 pL, a 1 pA current will deliver 3 μM cations per second. The current through the non-specific channels (ASIC and TRPC1) is carried mostly by extracellular Na^+ and it is in excess in ACSF. A partial current due to 1 mM NH^+_4 would then be (P_{NH4}. $[NH^+_4]/P_{Na}$. $[Na^+]$)·50 pA = 0.8 pA. This corresponds to the rate of NH^+_4 delivery ~2 μM/s, which is close to the estimate ~3 μM/s (Marcaggi & Coles, 2001) for transport rate for ammonia within the brain. This predicts that ~0.1 mM NH^+_4 could be accumulated in the cytoplasm during 30 s-long challenges to ammonia. Even if each NH^+_4 ion gives a proton away; it will be readily captured by intrinsic cytoplasmic pH buffers whose capacity is much bigger (~10 mM). This upper estimate of possible effect of NH^+_4 permeation indicate its marginal influence in our case. A conclusion is supported by the absence of changes in Ca^{2+} and HCN conductances, which should be depressed after presumable intracellular acidification by ammonia (Mironov & Lux, 1991; Zong et al., 2001).

Depolarization is an immediate response in neurons to NH_4^+. Seeking for appropriate subcellular candidates, we turned to non-specific cation channels, whose activation generates the inward current needed for depolarization. After blockade of TRPV1 channels, the activity of CA1 neurons and their responses to NH_4^+ were potentiated. Only the EPSC frequency was changed but not the amplitude (Fig. 8), therefore we tentatively ascribe the presynaptic actions of NH_4^+ upstream. TRPV1 channels endow hippocampal interneurons (Saffarzadeh et al., 2016), and therefore the removal of tonic inhibition of CA1 cells may explain a slight increase in excitability observed.

After blockade of ASIC (Fig. 4) and TRPC1 channels (Fig. 6), the glutamate spikes and neuronal bursts were suppressed and NH_4^+ responses diminished. In both cases we identified the changes as postsynaptic, because the blockers decreased only the EPSC amplitude but not the frequency (Figs. 4B and Fig. 6B). The exact location of ASIC and TRPC1 channels is difficult to discern at present. Most likely the channels are active in dendritic spines and cell soma. We can exclude their location in dendritic shafts, because the time course of EPSC measured in the

presence of blockers was not altered. Would the channels contribute to the dendritic conductance, changes in shunting would then modify EPSC kinetics; similar to what dendritic HCN channels do (Balakrishnan & Mironov, 2018a).

TRPC1 channels often colocalize with mGluR and the cross-talk between them is implicated in modulation of synaptic plasticity (Lepannetier et al., 2018). We previously described an important role of mGluR1/5 in RTT (Balakrishnan & Mironov, 2018). NH_4^+ effects in WT were markedly potentiated after mGluR1/5 stimulation (Fig. 7). Metabotropic glutamate receptors are invoked in inborn systemic hyperammonemia (Schrapers et al., 2018). This, and the important role of mGluR in determining a neuronal phenotype in RTT, suggests that NH_4^+ homeostasis can modulate a cross-talk between TRPC1 and mGluR1/5 and underlie significant aberrations during brain development.

The data add another piece of evidence to understanding possible origins of neuronal disturbances in RTT by first showing that ammonia strongly influences glutamate homeostasis. NH_4^+ effects are both immediate and long-lasting (Fig. 1). Elevation of ammonia within the brain may represent another factor that contributes to intrinsic overexcitability in RTT, whose symptoms develop during CNS maturation. The blood ammonia levels in RTT were measured in only one study (Campos-Castelló et al., 1988) and no significant changes were reported in 15 human patients. Perhaps it is premature to ultimately close the case and revive an original attribution of hyperammonemia to RTT (Rett, 1966). As argued in the Introduction backed by a recent literature (Seiler, 2002; Adlimoghaddam et al., 2016; Marcaggi & Coles, 2001), the local ammonia levels in the brain may not match those in blood plasma. Production and utilization of ammonia in neurons and glia can experience fast modification in interstitial ammonia levels. Measurement of ammonia within the brain is a challenging task. The measurements show that NH_4^+ modulates the activity of neurons within seconds. Ion-sensitive microelectrodes may not resolve such fast transients that can be also extremely localized. The imaging may help but reliable fluorescent probes are not yet designed.

The effects of ammonia in RTT are distinctly stronger. This might be expected, because RTT neurons are more excitable and glutamate handling is less efficient (Balakrishnan & Mironov, 2018a; Balakrishnan & Mironov, 2018b; Balakrishnan & Mironov, 2018). The inward currents generated by ASIC, TRPC1 and TRPV1 channels enhance depolarization drive to neurons and promote excitability. ASIC (Mironov & Lux, 1993) and TRPC1 channels (Balakrishnan & Mironov, 2018) are also permeable to Ca^{2+}. Our data posit these non-selective cation channels as important determinants in neuronal excitability.

It is logical to propose that intrinsic vulnerability of neurons in RTT and preponderance to epilepsy may be alleviated by respective blockers. A notion is supported by recent data about the role of ASIC and TRPC1 channels in the initiation and maintenance of seizures (Lepannetier et al., 2018). We must yet warn that a clinical usage of amiloride is to be made with caution, because this general ASIC channel blocker has also a weak stimulatory effect, similar to NH_4^+ itself (Adams et al., 1999); see also Fig. 4 in this study.

The data were obtained in hippocampus but may have more broad implications, because glutamatergic neurons are abundant in CNS and may respond to NH_4^+ in a similar way. Recent studies (Chepkova et al., 2017; Yanovsky et al., 2012) documented the effects of ammonia in the histaminergic neurons in hypothalamus in relation to mGluR1, ASIC and TRPC channels. It is proposed that the excitation is mediated by glutamate and is important in the control of arousal. This may also involve immediate increase in excitability by ammonia, similar to that observed in this study.

The observed effects might explain such acute ammonia actions as the historical use of smelling salts to arouse fainting persons or utilized today by power lifters and other athletes to get a burst of adrenaline before high intensity activities. Smelling salts help to arouse consciousness because ammonia gas first irritates the nose and lungs, and may cause an inhalation reflex. This alters the pattern of breathing, resulting in improved respiratory flow rates and possibly alertness due to adrenaline-inducing boost. In this study we examined CA1 hippocampal neurons and described a novel effect of their instant excitation by ammonia. The results obtained previously in DRG (Mironov & Lux, 1993) and cortical neurons (Pidoplichko & Dani, 2006) tempt to speculate that immediate reaction to ammonia may be stereotypical for many neuronal types including olfactory and sympathetic neurons. When nasal mucosa is irritated, the olfactory cortex would receive an adequate excitatory signal and process it with appropriate functional response. Direct or indirect stimulation of the second neuron in sympathicus would also increase subsequent secretion of catecholamines and stimulation of adrenergic receptors. On the downside, excessive cellular depolarization by ammonia may lead to neurotoxic effects, possibly explaining the link between local cerebral hyperammonia and cell death in diseases such as hepatic encephalopathy or Alzheimer's.

Author contributions

S.L.M: Conceptualization, Methodology, Data evaluation, Figures; Writing and funding acquisition. SB: Methodology, Patch-clamp and Imaging, Validation.

Funding

This project was funded by The Deutsche Forschungsgemeinschaft (DFG) through CNMPB (Centre for Nanoscale Microscopy and Molecular Physiology of the Brain, Cluster of Excellence 171, DFG Research Center 103, Germany).

Declaration of Competing Interest

The authors declare that the research was conducted in the absence of any commercial or financial relationships that could be construed as a potential conflict of interest.

Acknowledgements

We thank Nicole Hartelt for expert technical assistance. We also deeply appreciate the lab of Dr. Looger for sharing AAV-vector to express glutamate sensor in neurons and astrocytes.

Appendix A. Supplementary data

Supplementary data to this article can be found online at https://doi.org/10.1016/j.crphys.2020.05.002.

References

Adams, C.M., Snyder, P.M., Welsh, M.J., 1999. Paradoxical stimulation of a DEG/ENaC channel by amiloride. J. Biol. Chem. 274, 15500–15504.
Adlimoghaddam, A., Sabbir, M.G., Albensi, B.C., 2016. Ammonia as a potential neurotoxic factor in Alzheimer's disease. Front. Mol. Neurosci. 9, 57.
Bachmann, C., 2002. Mechanisms of hyperammonemia. Clin. Chem. Lab. Med. 40, 653–662.
Balakrishnan, S., Mironov, S.L., 2018. CA1 neurons acquire Rett Syndrome phenotype after brief activation of glutamatergic receptors: specific Role of mGluR1/5. Front. Cell. Neurosci. 12, 363–370.
Balakrishnan, S., Mironov, S.L., 2018a. Regenerative glutamate release in the hippocampus of Rett syndrome model mice. PloS One 13, e0202802.
Balakrishnan, S., Mironov, S.L., 2018b. Rescue of hyperexcitability in hippocampal CA1 neurons from Mecp2 (-/y) mouse through surface potential neutralization. PloS One 13, e0195094.
Burckhardt, B.C., Frömter, E., 1992. Pathways of NH_3/NH_4^+ permeation across Xenopus laevis oocyte cell membrane. Pflügers Archiv. 420, 83–86.
Cagnon, L., Braissant, O., 2007. Hyperammonemia-induced toxicity for the developing central nervous system. Brain Res. Rev. 56, 183–197.

Campos-Castelló, J., Peral Guerra, M., Riviere Gómez, A., Oliete García, F., Herranz Tanarro, J., Toledano Barrero, M., Espinar Sierra, J., Cristobal Sassot, S., Lautre Ecenarro, M.J., Franco Carcedo, C., et al., 1988. Rett's syndrome: study of 15 cases. An. Esp. Pediatr. 28, 286–292.

Chepkova, A.N., Sergeeva, O.A., Görg, B., Haas, H.L., Klöcker, N., Häussinger, D., 2017. Impaired novelty acquisition and synaptic plasticity in congenital hyperammonemia caused by hepatic glutamine synthetase deficiency. Sci. Rep. 7, 40190.

Dhaka, A., Uzzell, V., Dubin, A.E., Mathur, J., Petrus, M., Bandell, M., Patapoutian, A., 2009. TRPV1 is activated by both acidic and basic pH. J. Neurosci. 29, 153–158.

Guy, J., Hendrich, B., Holmes, M., Martin, J.E., Bird, A., 2001. A mouse Mecp2-null mutation causes neurological symptoms that mimic Rett syndrome. Nat. Genet. 27, 322–326.

Halpin, L.E., Northrop, N.A., Yamamoto, B.K., 2014. Ammonia mediates methamphetamine-induced increases in glutamate and excitotoxicity. Neuropsychopharmacology 39, 1031–1038.

Hille, B., 2001. Ion Channels of Excitable Membranes. Sinauer, Massachusetts.

Jardín, I., López, J.J., Diez, R., Sánchez-Collado, J., Cantonero, C., Albarrán, L., Woodard, G.E., Redondo, P.C., Salido, G.M., Smani, T., Rosado, J.A., 2017. TRPs in pain sensation. Front. Physiol. 8, 392–401.

Johnston, M.V., Ammanuel, S., O'Driscoll, C., Wozniak, A., Naidu, S., Kadam, S.D., 2014. Twenty-four hour quantitative-EEG and in-vivo glutamate biosensor detects activity and circadian rhythm dependent biomarkers of pathogenesis in Mecp2 null mice. Front. Syst. Neurosci. 8, 118–126.

Kitamura, N., Nagami, E., Matsushita, Y., Kayano, T., Shibuya, I., 2018. Constitutive activity of transient receptor potential vanilloid type 1 triggers spontaneous firing in nerve growth factor-treated dorsal root ganglion neurons of rats. IBRO Rep. 5, 33–42.

Leffler, A., Fischer, M.J., Rehner, D., Kienel, S., Kistner, K., Sauer, S.K., Gavva, N.R., Reeh, P.W., Nau, C., 2008. The vanilloid receptor TRPV1 is activated and sensitized by local anesthetics in rodent sensory neurons. J. Clin. Invest. 118, 763–776.

Lepannetier, S., Gualdani, R., Tempesta, S., Schakman, O., Seghers, F., Kreis, A., Yerna, X., Slimi, A., de Clippele, M., Tajeddine, N., Voets, T., Bon, R.S., Beech, D.J., Tissir, F., Gailly, P., 2018. Activation of TRPC1 channel by metabotropic glutamate receptor mGluR5 modulates synaptic plasticity and spatial working memory. Front. Cell. Neurosci. 12, 318.

Marcaggi, P., Coles, J.A., 2001. Ammonium in nervous tissue: transport across cell membranes, fluxes from neurons to glial cells, and role in signalling. Prog. Neurobiol. 64, 157–183.

Marvin, J.S., Borghuis, B.G., Tian, L., Cichon, J., Harnett, M.T., Akerboom, J., Gordus, A., Renninger, S.L., Chen, T.W., Bargmann, C.I., Orger, M.B., Schreiter, E.R., Demb, J.B., Gan, W.B., Hires, S.A., Looger, L.L., 2013. An optimized fluorescent probe for visualizing glutamate neurotransmission. Nat. Methods 10, 162–170.

Mironov, S.L., Langohr, K., 2007. Modulation of synaptic and channel activities in the respiratory network of the mice by NO/cGMP signalling pathways. Brain Res. 1130, 73–82.

Mironov, S.L., Lux, H.D., 1991. Cytoplasmic alkalinization increases high-threshold calcium current in chick dorsal root ganglion neurones. Pflügers Archiv. 419, 138–143.

Mironov, S.L., Lux, H.D., 1993. NH_4Cl-induced inward currents and cytoplasmic Ca^{2+} transients in chick sensory neurones. Neuroreport 4, 1055–1058.

Mironov, S.L., Langohr, K., Richter, D.W., 2000. Hyperpolarization-activated current, Ih, in inspiratory brainstem neurons and its inhibition by hypoxia. Eur. J. Neurosci. 12, 520–526.

Moretti, P., Zoghbi, H.Y., 2006. MeCP2 dysfunction in Rett syndrome and related disorders. Curr. Opin. Genet. Dev. 16, 276–281.

Nagaraja, T.N., Brookes, N., 1998. Intracellular acidification induced by passive and active transport of ammonium ions in astrocytes. Am. J. Physiol. 274, C883–C891.

Oja, S.S., Saransaari, P., Korpi, E.R., 2017. Neurotoxicity of ammonia. Neurochem. Res. 42, 713–720.

Pidoplichko, V.I., Dani, J.A., 2006. Acid-sensitive ionic channels in midbrain dopamine neurons are sensitive to ammonium, which may contribute to hyperammonemia damage. Proc. Natl. Acad. Sci. Unit. States Am. 103, 11376–11380.

Rangroo Thrane, V., Thrane, A., Wang, F., Cotrina, M.L., Smith, N.A., Chen, M., Xu, Q., Kang, N., Fujita, T., Nagelhus, E.A., Nedergaard, M., 2013. Ammonia triggers neuronal disinhibition and seizures by impairing astrocyte potassium buffering. Nat. Med. 19, 1643–1648.

Rett, A., 1966. On a unusual brain atrophy syndrome in hyperammonemia in childhood. Wien Med. Wochenschr. 116, 723–726.

Rose, C., Kresse, W., Kettenmann, H., 2005. Acute insult of ammonia leads to calcium-dependent glutamate release from cultured astrocytes, an effect of pH. J. Biol. Chem. 280, 20937–20944.

Saffarzadeh, F., Eslamizade, M.J., Mousav, i SM., Abraki, S.B., Hadjighassem, M.R., Gorji, A., 2016. TRPV1 receptors augment basal synaptic transmission in CA1 and CA3 pyramidal neurons in epilepsy. Neuroscience 314, 170–178.

Schrapers, K.T., Sponder, G., Liebe, F., Liebe, H., Stumpff, F., 2018. The bovine TRPV3 as a pathway for the uptake of Na^{+}, Ca^{2+}, and NH^{4+}. PloS One 13, e0193519.

Schroeter, A., Wen, S., Mölders, A., Erlenhardt, N., Stein, V., Klöcker, N., 2015. Depletion of the AMPAR reserve pool impairs synaptic plasticity in a model of hepatic encephalopathy. Mol. Cell. Neurosci. 68, 331–339.

Seiler, N., 2002. Ammonia and Alzheimer's disease. Neurochem. Int. 41, 189–207.

Szerb, J.C., Butterworth, R.F., 1992. Effect of ammonium ions on synaptic transmission in the mammalian central nervous system. Prog. Neurobiol. 39, 135–153.

Yamamoto, Y., Takahashi, Y., Imai, K., Mishima, N., Yazawa, R., Inoue, K., Itoh, K., Kagawa, Y., Inoue, Y., 2013. Risk factors for hyperammonemia in pediatric patients with epilepsy. Epilepsia 54, 983–989.

Yanovsky, Y., Zigman, J.M., Kernder, A., Bein, A., Sakata, I., Osborne-Lawrence, S., Haas, H.L., Sergeeva, O.A., 2012. Proton- and ammonium-sensing by histaminergic neurons controlling wakefulness. Front. Syst. Neurosci. 6, 23–31.

Zhang, L., He, J., Jugloff, D.G., Eubanks, J.H., 2008. The MeCP2-null mouse hippocampus displays altered basal inhibitory rhythms and is prone to hyperexcitability. Hippocampus 18, 294–309.

Zong, X., Stieber, J., Ludwig, A., Hofmann, F., Biel, M., 2001. A single histidine residue determines the pH sensitivity of the pacemaker channel HCN2. J. Biol. Chem. 276, 6313–6319.